Robust operation through effluent recycling for hydrogen production from the organic fraction of municipal solid waste

Florian Paillet, Carole Barrau, Renaud Escudié, Nicolas Bernet, Eric Trably

Robust operation through effluent recycling for hydrogen production from the organic fraction of municipal solid waste

Florian Paillet[a,b], Carole Barrau[a], Renaud Escudié[b], Nicolas Bernet[b], Eric Trably[b*]

[a] TRIFYL, Route de Sieurac, 81300 Labessiere-Candeil, France

[b] INRAE, Univ Montpellier, LBE, 102 avenue des Etangs, 11100, Narbonne, France

[*]Corresponding author: eric.trably@inrae.fr

Abstract

The stability of fermentative hydrogen production from the organic fraction of municipal solid waste (OFMSW) was evaluated in this work using a strategy of effluent recycling. Three pretreatment conditions were applied on the recycled effluent: a) no heat shock treatment, b) one initial heat shock treatment (90°C, 30 min) and c) systematic heat shock treatment at the beginning of each fermentation. When a systematic heat shock was applied, a maximal hydrogen yield of 17.2±3.*8* mLH_2/gVS was attained. The hydrogen productivity was improved by 331% reaching a stable value of 1.51±0.29 mLH_2/gVS/h, after 8 cycles of effluent recycling. This strategy caused a sharp decrease of diversity with stable co-dominance of hydrogen- and lactate-producing bacteria, ie. *Clostridiales* and *Lactobacillales*, respectively. For the other conditions, a sharp decrease of the hydrogen yields was observed showing the importance of applying a heat shock treatment for optimal hydrogen production with effluent recycling.

Keywords : Biohydrogen, Dark fermentation, Effluent recycling, Organic Fraction of Municipal Solid Waste, Stability

1. Introduction

The Organic Fraction of Municipal Solid Waste (OFMSW) is a highly available resource that can be valorized through biological processes such as dark fermentation. Over the past decade, hydrogen production by dark fermentation has been investigated as an interesting way of valorization, as H_2 is considered as an important carrier for the next-generation technologies (Dawood et al., 2020). However, one of the main limiting factors of fermentative biohydrogen production is the low yield of organic matter conversion that can make the process not economically reliable. To improve the viability of such process, the most interesting solution is to couple dark fermentation with anaerobic digestion, generating a mixture of H_2/CH_4 (5-20% of H_2) so-called Biohythane (Meena et al., 2020). Such coupling consists of a separation of acetogenesis/acidogenesis and methanogenesis making possible an optimization of each step for improving the total energy recovery. In addition, the hydrogen production in the first step does not have a significant negative impact on the methane yield compared to a single stage process, making hydrogen a pure gain of energy in the two-stage process (Hans and Kumar, 2019). Nonetheless, one limitation in coupling these two processes is the low total solid (TS) content to be applied in dark fermentation prior to the anaerobic digestion (*i.e.* methane production) step. As already reported, high hydrogen yields were observed for TS lower than 15% (Ghimire et al., 2018). In contrast, anaerobic digesters using OFMSW as substrate are usually operated at high TS content (>15%), in particular when solid-state anaerobic digestion technologies are implemented. In this context, the liquid part (so called "effluent") from dark fermentation could be removed to increase the TS of the substrate used for the anaerobic digestion. The collected effluent can here be recycled to the next fermentation step, which

47 is an interesting and innovative solution to supply in water the feeding of the first process.
48 Indeed, OFMSW are characterized by a low water content, with a TS of about 27.2±5.8%
49 (Campuzano and González-Martínez, 2016). In addition, effluent recycling can ensure the
50 inoculation of the dark fermenter with a well-adapted microbial community. Several studies
51 have already highlighted the positive impact of the use of effluent recirculation from a
52 methanogenic reactor to dark fermenter inoculation (O-Thong et al., 2016). In particular,
53 Zhang et al. (2007) showed the benefit of recirculating the methanogenic effluent on an
54 hydrolysis-acidogenic step by improving the total extracellular enzyme activities. This
55 strategy could be particularly adapted to dark fermentation by recycling the effluent after a
56 cycle of hydrogen production in discontinuous systems. However, effluent recirculation
57 may also promote the accumulation of soluble chemicals such as ammonia nitrogen, VFAs
58 and total ions that can hinder the hydrogen producing bacteria (Ariunbaatar et al., 2015;
59 Cavinato et al., 2012; Paillet et al., 2019). To avoid hydrogen consumption or the
60 development of non-H_2-producers bacteria, several physico-chemical pretreatments have
61 already been proposed such as a pH shock (Jang et al., 2015), a chemical treatment (Zhu
62 and Béland, 2006) or a heat shock treatment, the latter being the simplest, the less
63 expensive and the most effective method (Ghimire et al., 2015).
64 The aim of this study was to investigate different pretreatment conditions for recycling the
65 effluent of dark fermentation in successive batch reactors, in order to adapt the microbial
66 communities while avoiding inhibition of hydrogen production. Different modes of heat-
67 shock treatments were applied on the liquid phase (one initial heat shock and systematic
68 heat shock before each fermentation) to reduce the development of methanogens.

Accumulation of potential inhibitors was assessed to evaluate the long-term robustness of the dark fermentation process.

2. Materials and Methods

2.1. Feedstock and inoculum preparation

Organic Fraction of Municipal Solid Waste (OFMSW) was freshly prepared according to the average composition of OFMSW collected in France on a yearly basis (MODECOM™, 1993). The proportions of each component are described in Table 1. Meat, rice, potatoes and coffee grounds were cooked and mixed with yogurt and bread. Garden waste, paper and cardboards were shredded and sieved at 1 cm. Total solid (TS) and volatile solid (VS) contents of the freshly prepared OFMSW were 0.74±0.01 gTS/g and 0.63±0.01 gVS/g, respectively. The anaerobic inoculum corresponded to a sample of anaerobic lagoon treating leachates of methanogenic storage cells from a MSW landfill. The pH was 7.6, the conductivity 23.9±2.6 mS/cm, and the TS and VS contents were 0.0205±0.0003gTS/g and 0.0070±0.0002 gVS/g, respectively (NH_4^+: 2.4±0.2 g/L). Heat-shock treatment, was performed in a stirred bottle at 90°C for 30 min in order to inactivate methanogens (Ghimire et al., 2015).

2.2. Experimental set-up

All the experiments were carried out in a 6 L reactor made of polyvinyl chloride (PVC) manufactured for the study. Each batch reactor was performed at 37°C (Fisher scientific, Polystat 24, USA) and filled with 3 L of inoculum and 663.6 g (*i.e.*, 420.7 gVS) of freshly prepared OFMSW to obtain a total solid (TS) content of 15 %. Operating the fermenter at high solid contents increases productivity (mLH2/Lreactor/day), and reduces the amount of leachate addition. In accordance with preliminary tests, a TS content of 15% was selected

92 as it allows to obtain similar hydrogen yields at lower MS contents. pH was not regulated,
93 and the experiments were stopped when hydrogen accumulation stopped (3-4 days). The
94 first reactor of one initial heat shock experiment was operated for a longer time (5.3 days)
95 because hydrogen production was still detected at day 5. At the end of experiments, the
96 liquid fraction of the fermentate, called effluent, was sieved at 1mm and separated from the
97 solid fermentate. The effluent was then used for a new fermentation batch. Additional
98 leachate, stored in cold chamber (4°C), was added to the recycled effluent and the
99 OFMSW, to adjust the total volume at 3 L with a TS content of 15%.

100 **2.3. Process operation**

101 A schematic representation of the three experimental modes is provided in Fig. 1. A control
102 was carried out without any heat shock treatment during the experiments. Two different
103 modes of heat shock treatments were performed on the liquid phase. The condition named
104 "one initial heat shock" consisted of one unique heat treatment on the leachate used for the
105 first fermentation. The recycled effluent and the additional leachate for the next
106 fermentation were then used without any heat treatment. The condition named "systematic
107 heat shock" consisted to a systematic heat treatment of the liquid part of the dark fermenter.
108 This liquid part was composed of only leachate for the first fermentation cycle, and a
109 mixture of recycled effluent and additional leachate for the next cycles (Fig. 1). The ratio
110 corresponding to "additional leachate/effluent" was 51±8.3 % whatever the treatment
111 conditions, due to the similar feedstock applied in all experiments.
112 The control and the experiment with initial heat shock treatment were carried out on 6
113 successive batch reactors (6 cycles, 5 effluent recycling). The systematic heat shock
114 experiment was performed during 16 successive batch reactors (16 cycles, 15 effluent

115 recycling). For the three modes investigated, each reactor was named chronologically, eg.
116 the first reactor was called reactor n°1, second reactor n°2 etc. After each feeding operation,
117 the reactor headspace was purged with pure nitrogen gas to remove oxygen traces. 2 mL of
118 liquid phase was sampled and stored at -20°C at the beginning and at the end of each batch
119 for further analyses of metabolites and microbial composition. The pH, conductivity and
120 ammonia nitrogen concentration were measured at the beginning and at the end of each
121 batch.

122 **2.4. Analytical methods**

123 The gas composition was periodically measured (every 6 h) with an automated multiplexed
124 micro-gas chromatograph (µGC R3000, SRA instrument, France) equipped with two
125 analytical capillary columns to monitor on-line the gas production. The first column was
126 dedicated to carbon dioxide analysis (10 m length and 0.32 mm diameter) with argon as
127 carrier gas at a pressure of 30 PSI. The second column was dedicated to oxygen, hydrogen,
128 nitrogen and methane analysis (8 m length and 0.32 mm diameter) with helium as carrier
129 gas (20 PSI). The injector and column temperatures were 90°C and 80°C, respectively
130 (Motte et al., 2013). The total volume of gas produced was measured by a gas meter
131 (MilliGascounter® MGC-1, Ritter, Germany).
132 Metabolites were measured at the beginning (on the mixture of recycled effluent and
133 additional leachate) and at the end of each batch test, by using a high-performance liquid
134 chromatographic chain composed of an automatic sampler (Waters, 717 plus Autosampler),
135 a pre-column (Micro guard cation H refill cartbridges, Bio-rad) and a Aminex HPX-87
136 column set at 35°C. The carrier eluent corresponded to a 4mM sulfuric acid solution at a
137 flow rate of 0.4 $mL.min^{-1}$ (Motte et al., 2013).

2.5. Microbial community analysis

For microbial analyses, samples were collected at the end of each dark fermentation. DNA was extracted and purified with the Fast DNA SPIN kit for soil in accordance with manufacturer's instructions (MP Biomedicals). DNA quantity and purity were assessed by spectrophotometry (Infinite NanoQuant M200, Tecan). The V4 and V5 regions of the 16S rRNA genes were then amplified and sequenced by Illumina MiSeq (get.genotoul.fr) and sequences were analyzed.

2.6. Data analysis and calculation

Hydrogen production performances (i.e., hydrogen yield, maximal hydrogen production rate and lag phase) were calculated by fitting the cumulative hydrogen production curves with a modified Gompertz based-model (Eq. 1):

$$H(t) = H_{max} \times exp\left\{-exp\left[\frac{R_{max} \times e}{H_{max}}(\lambda - t) + 1\right]\right\} \quad \text{(Eq. 1)}$$

where H(t) is cumulative hydrogen volume (mL) at time t (h), H_{max} is the maximum hydrogen potential (mL), R_{max} is maximum hydrogen production rate (mL/h), λ is the lag-phase and e is the exp (1) = 2.718 . By considering the initial amount of VS in the substrate, it is possible to estimate the maximum hydrogen yield (mLH_2/gVS) and the maximum hydrogen productivity (mL H_2/gVS/h). The values of H_{max}, R_{max}, and λ were estimated using grofit R package (v 1.1.1-1).

All statistical analyses were performed with R software (v3.6.2) using RStudio (v1.2.5033). The "FactoMiner" (v2.1) package was used for PCA analysis, and the package "factoextra" (v1.0.6) for graphic visualization.

3. Results and discussion

160 **3.1. Hydrogen production**

161 Three parameters representative of hydrogen production performances, i.e. maximum
162 hydrogen yield (mLH_2/gVS), hydrogen lag phase (h) and maximum hydrogen productivity
163 ($mLH_2/gVS/h$) were estimated for each batch test. Fig. 2 presents these parameters over the
164 total duration of the experiments for the three different modes of recycled effluent
165 treatment: i) no heat shock, ii) one initial heat shock and iii) a systematic heat shock
166 treatment. For the mode with no treatment (control), the highest H_2 yield was observed
167 during the first batch cycle at 18.8 mLH_2/gVS and was close to the value reported by
168 Alibardi and Cossu. (2015) using OFMSW (~30±20 mLH_2/gVS). The production of
169 hydrogen varied significantly in the second and third reactors (H_2 yield of 10.8 and 15.9
170 mLH_2/gVS, respectively). The last three reactors (N°4, 5 and 6) showed a continuous
171 decrease of the H_2 yield. In the last reactor (*i.e.* after 5 cycles of effluent recycling), almost
172 no H_2 production was detected (0.4 mLH_2/gVS). Regarding the hydrogen lag phase, the
173 value measured in the first reactor was 22.4 h and decreased after the first effluent recycling
174 cycle reaching a constant value for the next reactors, at 7.5±0.5 h, which corresponded to a
175 reduction of 66.5%. In terms of hydrogen productivity, an unstable value was found
176 ranging from 0.57 to 1.23 $mLH_2/gVS/h$ during the first four reactors, before a drastic drop
177 for the last two batches at 0.20 and 0.03 $mLH_2/gVS/h$, respectively. For the mode
178 consisting of one initial heat shock treatment, a trend similar to the control was observed in
179 terms of H_2 yield. The best H_2 yield was observed in the first reactor with 10.5 mLH_2/gVS.
180 This value is slightly lower than in the control and can be explained by the inoculum
181 pretreatment that could negatively affect the production of hydrogen by generating stressful
182 conditions for the microbiota as reported by Luo et al., (2010). Then a continuous decrease

was observed until a low production for the last reactor (2.6 mLH_2/gVS). The hydrogen lag phase in the first reactor was 25.3 h and decreased after the first effluent recycling, reaching an average value of 7.9±2.0 h (reduction of 68.8%). When a systematic treatment was performed on the liquid phase (*i.e.* on the leachate used for the first reactor and then on the mixture of recycled effluent and additional leachate), a constant hydrogen production with an averaged value of 17.2±3.8 mLH_2/gVS was observed during 16 successive batch reactors. The average hydrogen yield measured was similar to the performances found in the literature for OFMSW when using heat shock treatment of the inoculum. In the study of Favaro et al. (2013), a production of hydrogen of 23.4±2.9 mLH_2/gVS was reported when heat shock treatment at 100°C for 4 h was applied using OFMSW (160±10 gTS/L). The lag phase was also very stable around 8.8±2.6 h. Interestingly, the maximum hydrogen productivity also increased from 0.35 $mLH_2/gVS/h$ from the first reactor to a stable value of 1.51±0.29 $mLH_2/gVS/h$ after 8 cycles of effluent recycling. Comparing the different treatment modes, no heat shock and one initial heat shock treatments showed a similar behavior with a global decrease of hydrogen production until almost no production after 6 successive batch cycles (H_2 yield of 0.4 and 2.6 mLH_2/gVS, respectively). With these two modes, methane was rapidly detected. Table 2 presents the time to reach the maximum hydrogen productivity and the time where significant methane accumulation was first detected. In the control, methane was detected after 51 h during the first batch. Thereafter, for reactors 4, 5 and 6, methane was produced at the same time than the maximum hydrogen productivity (17.7, 12.0 and 8.1 h, respectively). The decrease of hydrogen production can therefore be correlated with hydrogen consumption through methanogenesis (Ghimire et al., 2015). Four moles of hydrogen can theoretically be converted into one

206 mole of methane by hydrogenotrophic methanogens (Xu et al., 2019). For the mode
207 consisting in one initial heat shock, methane was also detected in the first batch but with a
208 longer delay (127.9 h) showing the benefit of heat shock treatment of the inoculum.
209 However, after the first effluent recycling, methane was produced faster (23.32 h) and
210 closer to the time of maximum hydrogen production. Thus, a heat shock treatment (90°C,
211 30 min) allowed to reduce the non-spore-forming microorganisms which consume
212 hydrogen, but with no complete elimination. Consistently, Luo et al. (2010) previously
213 reported that heat shock treatment (90°C for 1h) had only short-term effects on hydrogen
214 production performances. In comparison, in the case of systematic heat shock treatment, no
215 methane was observed all along the experiments, showing the robustness of such a strategy
216 to avoid hydrogen consumption by methanogens. Moreover, the heat shock treatment also
217 impacted the hydrogen productivity and its stability during the successive batch reactors.
218 Indeed, when no heat treatment was applied, low stability of hydrogen productivity was
219 observed with a decrease of the productivity correlated with the emergence of methane. As
220 soon as the heat shock treatment was used, as observed in the one initial heat shock
221 experiment, the maximum hydrogen productivity was low but more stable during the 6
222 successive batch reactors. A systematic heat shock treatment led to an increase of hydrogen
223 productivity, reaching a stable value of 1.51±0.29 mLH_2/gVS/h after 8 cycles of effluent
224 recycling (*i.e* from reactor 9), value being 331 % higher than the one found in the first dark
225 fermentation. Consistently, O-Thong et al. (2016) reported the benefit to recirculate the
226 effluent (with a recirculation rate of 30%) from methanogenic reactor into continuous
227 acidogenic reactor by improving the hydrogen productivity from 60 mLH_2/gCOD to 188
228 mLH_2/gCOD when compared to no recirculation.

229 The hydrogen lag phase was also positively impacted by effluent recycling. For the no heat
230 shock and the one initial heat shock treatment modes, the hydrogen lag phase was reduced
231 by 67.7±1.6 % after the first cycle of effluent recycling (i.e., between reactors 1 and 2). The
232 difference found between the one initial (25.3 h) and the systematic heat shock treatment
233 (10.1 h) was likely due to a difference in the amount of microorganisms and the microbial
234 activity between the used inocula, although the fermentation conditions were similar for
235 both experiments. However, whatever the treatment used, the lag phase reached a similar
236 value after the first effluent recycling, *i.e.* 7.5±0.5, 7.9±2.0 and 8.8±2.6 h for no heat shock,
237 one initial heat shock and systematic heat shock treatments, respectively. These values were
238 lower than the ones reported by Elbeshbishy et al. (2011) using heat shock treatment (70°C,
239 30 min) without effluent recycling strategy (16.3±1.6 h), which confirms the benefits of
240 recycling the effluent on the reduction and the stabilization of the lag phase.
241 Thus, the combination of effluent recycling and heat shock treatment of the liquid phase for
242 dark fermentation of OFMSW in successive batch reactors had a global positive impact on
243 all hydrogen performance indicators, such as H_2 yields, maximum productivity and lag
244 phase, and more especially when a systematic heat shock treatment was applied.

245 **3.2. Macroscopic parameters and inhibitors accumulation analysis**

246 Recycling the effluent can also promote the accumulation of soluble chemicals such as
247 VFAs, ions or ammonia which can subsequently affect the microbial activity and lead to
248 the inhibition of hydrogen production. The main parameters related to the chemicals
249 produced during dark fermentation were measured at the beginning (VFAs, pH,
250 conductivity) and at the end (pH, conductivity, Total Ammonia Nitrogen (TAN)) of each
251 reactor during the control (No), the one initial heat shock (One) and the systematic heat

252 shock (Syst) experiments (Fig. 3). The initial pH was similar for all the experiments
253 independently of the treatment method and number of effluent recycling cycles. The
254 average initial pH (Fig. 3A) was estimated at 7.0±0.5, 7.3±0.5 and 7.6±0.4 in the control,
255 the one initial heat shock and the systematic heat shock experiments, respectively. At the
256 end of fermentation, the pH was constant and lower than the initial pH (5.7±0.3, 5.4±0.4
257 and 5.5±0.2 for no heat shock, one initial heat shock and systematic heat shock
258 respectively). The final pH was consistent with similar experiment of dark fermentation
259 using kitchen waste as substrate (14.3 gVS/L) with a final pH measured at 5.88±0.04 when
260 the optimal hydrogen production was observed (Slezak et al., 2017). A high range of initial
261 pH, ie. from 5.0 to 9.0, has been reported for hydrogen production in batch dark
262 fermentation. Kim et al. (2011) observed a maximum for hydrogen production when the
263 initial pH was fixed at 8.0 (followed by a drop at pH 5) using food waste as substrate. A pH
264 lower than 5 can also affect hydrogen production as shown by Liu et al. (2006) during dark
265 fermentation of household solid waste. Consistently, the pH measured in the present
266 experiments was always in an optimal range for hydrogen production, decreasing from
267 7.6±0.4 to 5.5±0.2 over each batch operation. As a consequence, the decrease of hydrogen
268 performances observed in the control and the one initial heat shock method was not
269 correlated with of the pH variation. For control and systematic heat shock treatment modes,
270 an increase of the initial VFAs concentration was observed (Fig. 3B) from 16.2 and 44.2
271 mgCOD/gVS in reactor 1 to 105.1 and 123.0 mgCOD/gVS in reactor 6, respectively. In the
272 next successive batch reactors for the systematic heat shock experiment, an average and
273 stable value of 106±15 mgCOD/gVS was measured. In the one initial heat shock treatment
274 experiment, the concentration of initial VFAs was always lower than in the two other

modes (except for reactor 5 reaching similar value at 74.8 mgCOD/gVS). In the literature, it was found that a high initial content of VFAs can be detrimental to the microbial activity through the acidification of the medium resulting in a failure of the process (Ariunbaatar et al., 2015). It was reported that the undissociated forms of these acids (acetic or butyric acids) can cross the cell membrane and acidify the cellular medium by releasing protons during his dissociation, which implies an increase of the energy demand to maintain constant the internal pH. Here, the improvement of the overall hydrogen performances in the systematic heat shock experiment (reduction of hydrogen lag phase and increase of productivity) showed that the initial VFA concentration was not detrimental to hydrogen production. As well, the inhibition of hydrogen production observed in the control and during the one initial heat shock treatment experiment was not correlated to the VFA accumulation since the concentrations found for these two conditions were close to the systematic heat shock treatment experiment. The stability of the initial VFA concentration can be easily linked to the potential of water absorption of the organic matter during fermentation. After each dark fermentation, the liquid phase (called "effluent") was separated from the solid phase by sieving, the quantity of effluent collected allow to know the amount of liquid absorbed in the 'fermentate' (*i.e.* solid phase). Thus, it was measured that an average of 51±8.3 % the liquid phase was absorbed in the solid phase whatever the operation mode (mainly due to the presence of paper and cardboard). As a consequence, and in addition to the effluent recycled for the next dark fermenter, additional leachate has to be incorporated to maintain similar conditions along the experiments (TS of 15%), leading to a dilution and a stabilization of the VFAs concentration.

297 Ionic strength is also known to have a detrimental effect on hydrogen production, as
298 already reported elsewhere (Paillet et al., 2019). In the present study, the conductivity,
299 which is correlated to the total ionic strength, remained constant during the entire duration
300 of the experiments, whatever the operation mode (control, one initial heat shock and
301 systematic heat shock treatment), showing no accumulation of inhibitory ions in the
302 medium (Fig. 3.C). Finally, as reported in Fig. 3.D, no accumulation of ammonia nitrogen
303 (TAN) was detected. For the systematic and one initial heat shock treatment experiment, a
304 similar trend was observed with average final concentrations of 2.1±0.4 gN/L and 2.1±0.2
305 gN/L respectively. In the control, from reactor 1 to 3, a slight increase of TAN was
306 observed from 2.42 to 3.1 gN/L to reach a stable phase until a drop at 2.1 gN/L for the last
307 reactor. According to the literature, the concentrations observed in the present study were in
308 an adequate range for hydrogen production and not associated to ammonia inhibition.
309 Indeed, Pan et al. (2013) showed an inhibition of hydrogen production for TAN
310 concentration higher than 3.5 gN/L. Thus, from the macroscopic parameters analysis, the
311 main reasons for the decline of hydrogen production is not due to the accumulation of
312 inhibitors when effluent recycling strategy is applied.

313 **3.3. Metabolite production**

314 Based on the initial and final concentrations of metabolites (VFAs, lactate, ethanol,
315 butanol), the efficiency of production of metabolites in dark fermentation was estimated.
316 The average COD of metabolites produced per fermentation was 142.8±21.4, 109.1±27.3
317 and 131.4±27.5 mgCOD/gVS for no heat shock, one initial heat shock and systematic heat
318 shock treatment experiments, respectively. The metabolites produced were in the same
319 range than the values usually found in dark fermentation of organic waste (140.7±23

320 mgCOD/gVS) (Ghimire et al., 2018). This suggests an efficient microbial activity in each
321 reactor and that heat shock treatment and effluent recycling did not impact the global
322 microbial conversion of OFMSW into metabolites. The distribution of metabolites
323 produced during each fermentation are presented in Fig. 4 for the three treatment modes. In
324 the control condition, the main metabolites produced during the first reactor were acetate
325 and butyrate, representing 23.0% and 60.7% of the total COD, respectively (*i.e.* 33.5 and
326 88.3 mgCOD/gVS, respectively). After the first effluent recycling, other metabolites were
327 produced such as lactate (34.2 and 12.4 mgCOD/gVS for reactors 2 and 3, respectively) or
328 caproate that gradually increased in proportion, from 6.1%$_{COD}$ to 32.6%$_{COD}$ between reactor
329 1 and 6. The metabolite shift observed between the production of lactate and caproate can
330 be explained by elongation chain mechanisms (Han et al., 2019). As demonstrated by Zhu
331 et al.(2015), lactate can be used as electron donor for the synthesis of medium-chain
332 carboxylic acids (MCCAs) as caproate under anaerobic fermentative conditions by
333 *Clostridium* sp. The proportion of valerate also increased from 5.7%$_{COD}$ in reactor 4 to
334 14.0%$_{COD}$ in reactor 6. Overall, the recycling strategy with no heat treatment showed a
335 modification of the selected metabolic pathways with the emergence of lactate, caproate
336 and valerate at the detriment of butyrate. In the one initial heat shock mode, the two main
337 metabolites found in the first reactor were acetate and butyrate at a proportion of 37.1%$_{COD}$
338 and 49.5%$_{COD}$, respectively. After the first cycle of effluent recycling, the proportions of
339 acetate and butyrate decreased and a new metabolite, ie. Caproate, was detected in a
340 significant proportion. Caproate reached 10.2±3.5 %$_{COD}$ at the end of fermentation in the
341 reactors 2, 3 and 4. Significant lactate accumulation was also observed, from 28.7%$_{COD}$ to
342 57.0%$_{COD}$ in reactors 2 and 6, respectively. Compared to the control, lactate was

343 continuously produced after the first effluent recycling and became the main metabolite
344 produced. Thus, one initial heat shock condition likely stabilized the metabolic pathways by
345 promoting the production of lactate. In the systematic heat shock treatment mode, the main
346 metabolite was butyrate, with a proportion ranging from 26.4%$_{COD}$ to 63.5%$_{COD}$. Acetate
347 and ethanol (except in reactor 11) were also produced constantly (10.6±2.7 %$_{COD}$ and
348 10.1±5.6 %$_{COD}$ respectively). The other metabolites such as propionate, caproate, lactate
349 and butanol, were produced with higher variability. Butanol appeared in 8 reactors out of
350 16 and lactate in 12 out of 16 with a high standard deviation (*i.e.* 16.2±11.0 %$_{COD}$) showing
351 the instability in the production of these metabolites in the systematic heat shock treatment
352 condition. In dark fermentation, the two main metabolic pathways producing hydrogen are
353 the acetate and butyrate pathways and these two metabolites are the main end products
354 (Cavinato et al., 2012). Consistently, in the present study, the best hydrogen yields
355 observed during no heat shock and one initial heat shock conditions (18.8 mLH_2/gVS and
356 10.5 mLH_2/gVS, respectively) were obtained in the first reactor, when the overall
357 proportion of acetate and butyrate represented 83.6%$_{COD}$ and 86.6%$_{COD}$ of the total
358 metabolites, respectively. Interestingly, high concentration of butyric acid can inhibit the
359 activity of methanogens as already discussed by Li et al., (2018), which could be another
360 explanation of the delay observed for the development of methanogens. In the systematic
361 heat shock treatment condition, the accumulation of these two metabolites and especially
362 butyrate was in line with the constant production of hydrogen. In addition, the butyrate to
363 acetate ratio (B/A) can reflect the theoretical hydrogen yield. In particular, with a ratio B/A
364 of 1.5, it was suggested a hydrogen yield of 2.5 molH_2/mol$_{hexose}$ (Hawkes et al., 2007). In
365 this study, the B/A ratio was 1.48±0.51 and 1.47±0.54 for no heat shock and systematic

366 heat shock treatment conditions, respectively, while for one initial heat shock treatment, the
367 ratio was lower (0.80±0.30) mainly caused by the decrease of butyrate production.
368 Several metabolic pathways enter also in competition with hydrogen production since they
369 do not generate hydrogen during the conversion of organic matter which is an additional
370 reason of hydrogen inhibition. For instance, propionate, caproate and lactate pathways are
371 the mostly found non-hydrogen producing pathways (Motte et al., 2013). Thus, the
372 decrease of butyrate, correlated with the emergence of valerate, caproate and lactate, is an
373 additional explanation for the low production of hydrogen observed in no heat shock and
374 one initial heat shock conditions. However, regarding the B/A ratio of these two modes, the
375 low production of hydrogen during the no heat shock experiment was mainly caused by
376 hydrogenotrophic methanogens since theB/A ratio (1.48±0.51) was closed to the optimal
377 value. Whereas, in one initial heat shock condition, the lower ratio of B/A (0.80±0.30)
378 showed a stronger selection of competitive metabolic pathways of hydrogen production,
379 especially lactate. Thus, one initial heat shock condition could be a short-term solution to
380 avoid hydrogen consumption through methanogenesis but the effluent recycling strategy
381 seems to promote the competitive metabolic pathways of hydrogen production.
382 Interestingly, ethanol and butanol were also produced in significant proportions during
383 systematic heat shock treatment mode (10.6±2.7 %COD and 10.1±5.6 %COD,
384 respectively). Xue & Cheng (2019) showed that *Clostridium* sp., which are the major
385 sporulating hydrogen-producing bacteria, can also produce butanol and ethanol via ABE
386 (acetone-butanol-ethanol) fermentation, by solventogenesis. The solventogenic pathway
387 refers to the assimilation of acids to produce solvents. To better understand the impact of
388 these metabolites on the overall process, a principal component analysis (PCA) was

389 performed (Fig. 5) and shows that hydrogen production was negatively correlated to
390 ethanol and butanol production suggesting that these two molecules were not involved in
391 hydrogen production pathways. This is consistent with the study of Kim et al. (2011) who
392 showed that, when the environmental conditions are favorable for hydrogenases, oxidized
393 by-products such as acetate and butyrate, are concomitantly produced with hydrogen. In
394 contrast, when hydrogenases are inhibited the production of ethanol and butanol pathways
395 are favored. As reported in the literature, high partial pressure of hydrogen is a cause of
396 changes in metabolic pathways towards the production of lactate, acetone, butanol and
397 ethanol (Levin, 2004). As already discussed above, inoculum pretreatment could also
398 negatively affect the production of hydrogen by generating stressful conditions for the
399 microbiota. Finally, the consumption of hydrogen by homoacetogenesis (4 moles of
400 hydrogen to produced 1 mole of acetate) can be one of the main factors of hydrogen
401 consumption resulting in the production of acetate (Saady, 2013). Fig. 5 shows a negative
402 correlation between acetate and hydrogen production which suggests that
403 homoacetogenesis could have occured during the experiment. However, no increase of
404 acetate proportion within the produced metabolites was observed, suggesting that the
405 effluent recycling strategy did not favor the development of homoacetogenic bacteria.
406 Consistently, systematic heat shock treatment coupled to effluent recycling likely favored a
407 continuous selection of microbial populations carrying metabolic pathways related to
408 hydrogen production (mainly butyrate) and avoided hydrogen consumption by
409 methanogens. The emergence of alternative metabolic pathways (butanol, ethanol, lactate)
410 was probably a sign of microbial community stress.

3.4. Development of the fermentative microbial communities during effluent recycling for successive batch reactors

The microbial community at the beginning of each batch reactor corresponded to the microbial community of the heat pretreated inoculum (mixture of leachate and recycling effluent after the first reactor), whereas it corresponded to the fermented medium at the end of each batch reactor. Analysis of the microbial community was performed in samples collected at the beginning (7 samples) and at the end (13 samples) of the successive batch reactors, operated with systematic heat shock treatment. Considering all the samples, a total of 1082 operating taxonomic units (OTUs) were found. The most dominant taxonomic orders at start of the reactors (Fig. 6 A) were affiliated to *Pseudomonadales* (with an abundance ranging from 3% to 46% of the total sequences), *Clostridiales* (abundance from 5% to 51%), *Lactobacillales* (6 to 25%) and *Bacillales* (0 to 33%). Higher diversity was found at start of the first reactors (reactor 1 to 7) with an important proportion of *Pseudomonalades* and *Bacillales.* A shift of the microbial community was then observed, with the dominance of *Clostridiales* and *Lactobacillales* showing good stability on the microbial community from reactor 8 to 16. The samples collected at the end of fermentation showed a very stable community structure all along the experiment with two dominant taxonomic orders, *Clostridiales* and *Latobacillales*, with relative abundances ranging from 37 to 63% and from 5% to 60%, respectively (Fig. 6B). Only in the first reactor, the presence of *Bacillales* (24% of relative abundance) was observed. Then, the *Clostridiales* maintained his population compared to the initial leachate composition while the proportion of *Lactobacillales*, initially present at 6.8%, increased largely and outcompeted the other species. The systematic decrease of microbial diversity identified at

434 the end of fermentation is consistent with previous observations of Yang & Wang, (2019)
435 who showed a similar microbial diversity decrease during dark fermentation with only four
436 different dominant genera after fermentation : *Clostridium sp.*, *Paraclostridium*,
437 *Romboustia* and *Paeniclostridium*. By performing a BLASTn search using the NCBI
438 database, at the end of fermentation, the most abundant OTUs issued from *Clostridiales*
439 (37±8% of total relative abundance) could be affiliated to two species with close similarity
440 (97% 16S rRNA sequence similarity): *Clostridium butyricum* or *Clostridium beijerinckii*.
441 These two species have been widely described as efficient hydrogen-producing bacteria.
442 Liu et al. (2011) reported a high hydrogen production with *Clostridium butyricum* (1.77
443 $mmol/mmol_{glucose}$) and *Clostridium beijerinckii* (1.72 $mmol/mmol_{glucose}$) in pure cultures.
444 *Clostridium butyricum* produces mainly butyrate which can explain the high butyrate
445 production found in the systematic heat shock treatment condition (Cheng et al., 2011).
446 Concerning the *Lactobacillales* order, the diversity was mainly represented by three main
447 species. The most abundant one (16±11%) was affiliated to *Lactobacillus mucosae* or
448 *Lactobacillus spicheri* (98% 16S rRNA sequence similarity). These species were already
449 described as lactate producers (Meroth et al., 2004). The two other species had a slightly
450 lower relative abundance of 9±8% and 5±4%, and were affiliated to *Lactobacillus*
451 *plantarum* (100% rRNA sequence similarity) and *Lactobacillus paracasei* or *Lactobacillus*
452 *casei* (100% rRNA sequence similarity), respectively, also known as lactate producers
453 (Chen et al., 2020; Kuo et al., 2015). The lactate producers are well known to outcompete
454 hydrogen producing bacteria. Interestingly, in the present experiment, an equilibrium was
455 observed between *Lactobacillales* and *Clostridiales*. Some species of *Clostridium sp.* such
456 as *C. beijerinckii* and *C. butyricum* are able to consume lactate and acetate to produce

butyrate and hydrogen (García-Depraect et al., 2019). Interestingly, these two species were found after fermentation with a high proportion of butyrate. Moreover, lactate concentration showed a high variability (*i.e.* 16.2±11.0 $\%_{COD}$) even though *Lactobacillales* were abudant. All this suggests that lactate was partially consumed along the fermentation process. From the metabolite distribution (Fig. 4), both the production of butyrate and lactate was highly variable. In particular, when a high proportion of lactate was detected, a low proportion of butyrate was observed and vice-versa, supporting the probable link between these two pathways. Consistently, the PCA (Fig. 5) analysis showed that lactate negatively correlated to butyrate, corroborating to this assumption. Due to the fact that lactate is involved in a no H_2 producing (product) or a producing hydrogen pathways (substrate), no clear correlation was observed with hydrogen. Since it influenced the statistical test, butyrate did not clearly positively correlate to hydrogen production.

4. Conclusion

The stability of hydrogen production in a dark fermentation reactor using different effluent recycling strategies was investigated. Optimal performances were obtained when heat shock treatment was systematically applied on the recycled effluent, at the beginning of each fermentation. Indeed, by recycling the effluent a reduction of the lag phase was observed and the use of systematic heat shock treatment enhanced the hydrogen productivity and stabilized the hydrogen yield. In this study, relevant operating conditions are proposed to sustain robust and constant hydrogen production from the complex OFMSW, as a new opportunity for producing green hydrogen at larger scale.

References

1. Alibardi, L., Cossu, R., 2015. Composition variability of the organic fraction of municipal solid waste and effects on hydrogen and methane production potentials. Waste Manag. 36, 147–155.

2. Ariunbaatar, J., Scotto Di Perta, E., Panico, A., Frunzo, L., Esposito, G., Lens, P.N.L., Pirozzi, F., 2015. Effect of ammoniacal nitrogen on one-stage and two-stage anaerobic digestion of food waste. Waste Manag. 38, 388–398.

3. Campuzano, R., González-Martínez, S., 2016. Characteristics of the organic fraction of municipal solid waste and methane production: A review. Waste Manag. 54, 3–12.

4. Cavinato, C., Giuliano, a., Bolzonella, D., Pavan, P., Cecchi, F., 2012. Bio-hythane production from food waste by dark fermentation coupled with anaerobic digestion process: A long-term pilot scale experience. Int. J. Hydrogen Energy 37, 11549–11555.

5. Chen, P.-T., Hong, Z.-S., Cheng, C.-L., Ng, I.-S., Lo, Y.-C., Nagarajan, D., Chang, J.-S., 2020. Exploring fermentation strategies for enhanced lactic acid production with polyvinyl alcohol-immobilized Lactobacillus plantarum 23 using microalgae as feedstock. Bioresour.Technol. 308, 123266.

6. Cheng, C.-H., Hsu, S.-C., Wu, C.-H., Chang, P.-W., Lin, C.-Y., Hung, C.-H., 2011. Quantitative analysis of microorganism composition in a pilot-scale fermentative biohydrogen production system. Int. J. Hydrogen Energy 36, 14153–14161.

7. Dawood, F., Anda, M., Shafiullah, G.M., 2020. Hydrogen production for energy: An overview. Int. J. Hydrogen Energy 45, 3847–3869.

8. Elbeshbishy, E., Hafez, H., Dhar, B.R., Nakhla, G., 2011. Single and combined effect of various pretreatment methods for biohydrogen production from food waste. Int. J. Hydrogen Energy 36, 11379–11387.

502 9. Favaro, L., Alibardi, L., Lavagnolo, M.C., Casella, S., Basaglia, M., 2013. Effects of
503 inoculum and indigenous microflora on hydrogen production from the organic fraction of
504 municipal solid waste. Int. J. Hydrogen Energy 38, 11774–11779.
505 10. García-Depraect, O., Valdez-Vázquez, I., Rene, E.R., Gómez-Romero, J., López-López,
506 A., León-Becerril, E., 2019. Lactate- and acetate-based biohydrogen production through
507 dark co-fermentation of tequila vinasse and nixtamalization wastewater: Metabolic and
508 microbial community dynamics. Bioresour. Technol. 282, 236–244.
509 11. Ghimire, A., Frunzo, L., Pirozzi, F., Trably, E., Escudie, R., Lens, P.N.L., Esposito, G.,
510 2015. A review on dark fermentative biohydrogen production from organic biomass:
511 Process parameters and use of by-products. Applied Energy 144, 73–95.
512 12. Ghimire, A., Trably, E., Frunzo, L., Pirozzi, F., Lens, P.N.L., Esposito, G., Cazier,
513 E.A., Escudié, R., 2018. Effect of total solids content on biohydrogen production and lactic
514 acid accumulation during dark fermentation of organic waste biomass. Bioresour. Technol.
515 248, 180–186.
516 13. Han, W., He, P., Shao, L., Lü, F., 2019. Road to full bioconversion of biowaste to
517 biochemicals centering on chain elongation: A mini review. J. Environ. Sciences 86, 50–64.
518 14. Hans, M., Kumar, S., 2019. Biohythane production in two-stage anaerobic digestion
519 system. Int. J. Hydrogen Energy 44, 17363–17380.
520 15. Hawkes, F., Hussy, I., Kyazze, G., Dinsdale, R., Hawkes, D., 2007. Continuous dark
521 fermentative hydrogen production by mesophilic microflora: Principles and progress. Int. J.
522 Hydrogen Energy 32, 172–184.
523 16. Jang, S., Kim, D.-H., Yun, Y.-M., Lee, M.-K., Moon, C., Kang, W.-S., Kwak, S.-S.,
524 Kim, M.-S., 2015. Hydrogen fermentation of food waste by alkali-shock pretreatment:

525 Microbial community analysis and limitation of continuous operation. Bioresour. Technol.
526 186, 215–222.
527 17. Kim, D.H., Kim, S.H., Jung, K.W., Kim, M.S., Shin, H.S., 2011. Effect of initial pH
528 independent of operational pH on hydrogen fermentation of food waste. Bioresour.
529 Technol. 102, 8646–8652.
530 18. Kuo, Y.-C., Yuan, S.-F., Wang, C.-A., Huang, Y.-J., Guo, G.-L., Hwang, W.-S., 2015.
531 Production of optically pure l -lactic acid from lignocellulosic hydrolysate by using a newly
532 isolated and d -lactate dehydrogenase gene-deficient Lactobacillus paracasei strain.
533 Bioresour. Technol. 198, 651–657.
534 19. Levin, D., 2004. Biohydrogen production: prospects and limitations to practical
535 application. Int. J. Hydrogen Energy 29, 173–185.
536 20. Li, Z., Chen, Z., Ye, H., Wang, Y., Luo, W., Chang, J.-S., Li, Q., He, N., 2018.
537 Anaerobic co-digestion of sewage sludge and food waste for hydrogen and VFA production
538 with microbial community analysis. Waste Manag. 78, 789–799.
539 21. Liu, Dawei, Liu, Dapeng, Zeng, R.J., Angelidaki, I., 2006. Hydrogen and methane
540 production from household solid waste in the two-stage fermentation process. Water
541 research 40, 2230–2236.
542 22. Liu, I.-C., Whang, L.-M., Ren, W.-J., Lin, P.-Y., 2011. The effect of pH on the
543 production of biohydrogen by clostridia: Thermodynamic and metabolic considerations.
544 Int. J. Hydrogen Energy 36, 439–449.
545 23. Luo, G., Xie, L., Zou, Z., Wang, W., Zhou, Q., 2010. Evaluation of pretreatment
546 methods on mixed inoculum for both batch and continuous thermophilic biohydrogen
547 production from cassava stillage. Bioresour. Technol. 101, 959–964.

548 24. Meena, R.A.A., Rajesh Banu, J., Yukesh Kannah, R., Yogalakshmi, K.N., Kumar, G.,
549 2020. Biohythane production from food processing wastes – Challenges and perspectives.
550 Bioresour. Technol. 298, 122449.
551 25. Meroth, C.B., Hammes, W.P., Hertel, C., 2004. Characterisation of the Microbiota of
552 Rice Sourdoughs and Description of Lactobacillus spicheri sp. nov. Syst. Appl.
553 Microbiology 27, 151–159.
554 26. Motte, J.-C., Trably, Eric., Escudié, Renaud., Hamelin, J., Steyer, J.-P., Bernet, N.,
555 Delgenes, J.-P., Dumas, C., 2013. Total solids content: a key parameter of metabolic
556 pathways in dry anaerobic digestion. Biotech. for biofuels 6, 164.
557 27. O-Thong, S., Suksong, W., Promnuan, K., Thipmunee, M., Mamimin, C., Prasertsan,
558 P., 2016. Two-stage thermophilic fermentation and mesophilic methanogenic process for
559 biohythane production from palm oil mill effluent with methanogenic effluent recirculation
560 for pH control. Int. J. Hydrogen Energy 41, 21702–21712.
561 28. Paillet, F., Barrau, C., Escudié, R., Trably, E., 2019. Inhibition by the ionic strength of
562 hydrogen production from the organic fraction of municipal solid waste. Int. J. Hydrogen
563 Energy 45. 5854-5863
564 29. Pan, J., Chen, X., Sheng, K., Yu, Y., Zhang, C., Ying, Y., 2013. Effect of ammonia on
565 biohydrogen production from food waste via anaerobic fermentation. Int. J. Hydrogen
566 Energy 38. 12747–12754.
567 30. Saady, N.M.C., 2013. Homoacetogenesis during hydrogen production by mixed
568 cultures dark fermentation: Unresolved challenge. Int. J. Hydrogen Energy 38, 13172–
569 13191.

570 31. Slezak, R., Grzelak, J., Krzystek, L., Ledakowicz, S., 2017. The effect of initial organic
571 load of the kitchen waste on the production of VFA and H2 in dark fermentation. Waste
572 Manag. 68, 610–617.
573 32. Xu, R., Xu, S., Florentino, A.P., Zhang, L., Yang, Z., Liu, Y., 2019. Enhancing
574 blackwater methane production by enriching hydrogenotrophic methanogens through
575 hydrogen supplementation. Bioresour. Technol. 278, 481–485.
576 33. Xue, C., Cheng, C., 2019. Butanol production by Clostridium. Adv. in Bioenergy 4, 35–
577 77.
578 34. Yang, G., Wang, J., 2019. Changes in microbial community structure during dark
579 fermentative hydrogen production. Int. J. Hydrogen Energy 44, 25542–25550.
580 35. Zhang, B., He, P.J., Lü, F., Shao, L.M., Wang, P., 2007. Extracellular enzyme activities
581 during regulated hydrolysis of high-solid organic wastes. Water Research 41, 4468–4478.
582 36. Zhu, H., Béland, M., 2006. Evaluation of alternative methods of preparing hydrogen
583 producing seeds from digested wastewater sludge. Int. J. Hydrogen Energy 31, 1980–1988.
584 37. Zhu, X., Tao, Y., Liang, C., Li, X., Wei, N., Zhang, W., Zhou, Y., Yang, Y., Bo, T.,
585 2015. The synthesis of n-caproate from lactate: a new efficient process for medium-chain
586 carboxylates production. Sci Rep 5, 14360.
587
588
589
590
591

592 **Fig. 1** : Schematic representation of the three different conditions (heat treatment and
593 effluent recirculation) used for successive batch dark fermenters.
594 **Fig. 2** : Hydrogen production performances (maximum yield ■, maximum productivity ■
595 and lag phase •) from dark fermentation of OFMSW using different heat shock treatment
596 conditions (no heat shock, one initial heat shock and systematic heat shock).
597 **Fig. 3** : Evolution of pH, total volatile fatty acids concentration (VFAs), conductivity and
598 Total Ammonia Nitrogen (TAN) for the three heat shock treatment conditions (no heat
599 shock – No; one initial heat shock - One; systematic heat shock -Syst).
600 **Fig. 4** : Metabolite distribution and total COD production (gCOD/gVS) in dark
601 fermentation batch reactors using different heat shock treatment conditions (no heat shock,
602 one-time heat shock and systematic heat shock).
603 **Fig. 5** : PCA of the performances of effluent recirculation reactors for systematic heat
604 shock treatment, H2: hydrogen yield (mLH_2/gVS).
605 **Fig. 6** : Relative abundance of microbial communities at the start (A) and at the end (B) of
606 dark fermentations during systematic heat shock condition.
607 **Table 1** : Composition of the freshly prepared OFMSW. Data are reported as percentage on
608 wet weight basis (% w/w)
609 **Table 2** : Time to reach the maximum of hydrogen productivity (in h) and the time of first
610 significant methane detection (in h) during the three experiments (no heat shock, one initial
611 heat shock and systematic heat shock)
612
613

Category	Elements	% w/w	TS (gTS/g)	VS (gVS/g)
Food waste	Meat	7.0	0.45±0.01	0.43±0.01
	Coffee grounds	3.9	0.32±0.01	0.32±0.01
	Rice	4.3	0.28±0.01	0.27±0.01
	Potatoes	20.9	0.26±0.01	0.24±0.01
	Bread	5.1	0.96±0.01	0.95±0.01
	Yogurt	2.0	0.13±0.01	0.12±0.01
Garden waste	Grass	5.0	0.28±0.01	0.25±0.01
Paper	Office paper	31.7	0.94±0.01	0.76±0.01
Cardboard	Moving cardboard	16.7	0.92±0.01	0.77±0.01
	Paper folder	3.4	0.94±0.01	0.91±0.02

Table 1

	Reactor N°	1	2	3	4	5	6	7	8	9	10	11	12	13	14	15	16
No heat shock	tH_2 max (h)	29.7	22.8	15.1	14.7	12.0	20.1										
	tCH_4 (h)	50.7	79.8	42.1	17.7	12.0	8.1										
One initial heat shock	tH_2 max (h)	31.9	16.0	12.0	16.0	16.0	16.0										
	tCH_4 (h)	127.9	23.3	16.0	16.0	12.0	12.0										
Systematic heat shock	tH_2 max (h)	26.0	16.6	10.0	14.1	15.0	15.0	18.0	24.0	21.1	12.7	15.8	12.0	13.9	12.0	24.1	48.0
	tCH_4 (h)	0	0	0	0	0	0	0	0	0	0	0	0	0	0	0	0

Table 2

Fig. 1.

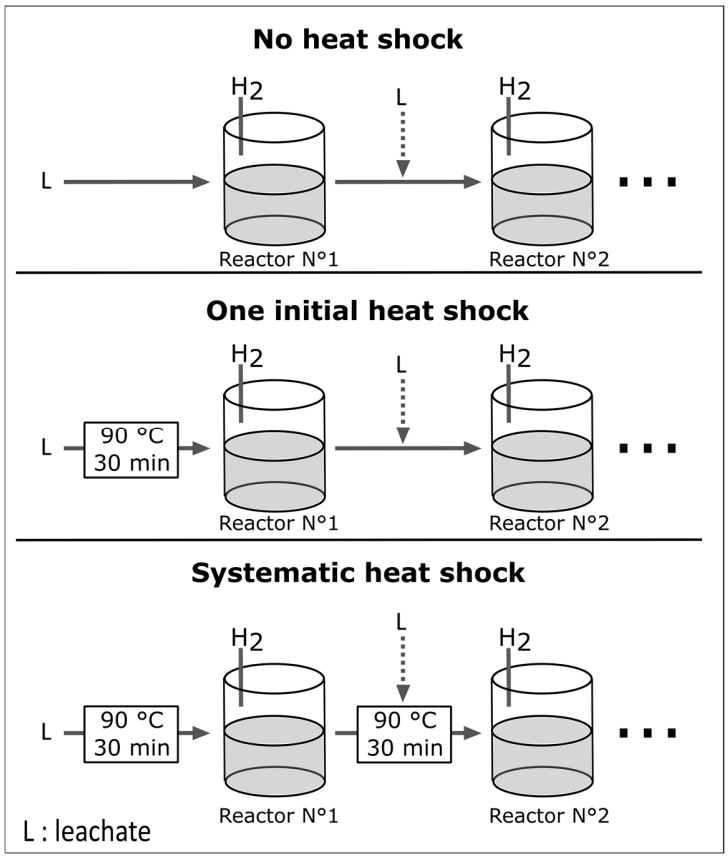
No heat shock
H2
L
H2
L
Reactor N°1
Reactor N°2
One initial heat shock
H2
L
H2
L
90 °C
30 min
Reactor N°1
Reactor N°2
Systematic heat shock
L
H2
H2
L
90 °C
30 min
90 °C
30 min
Reactor N°1
Reactor N°2
L : leachate

Fig. 2.

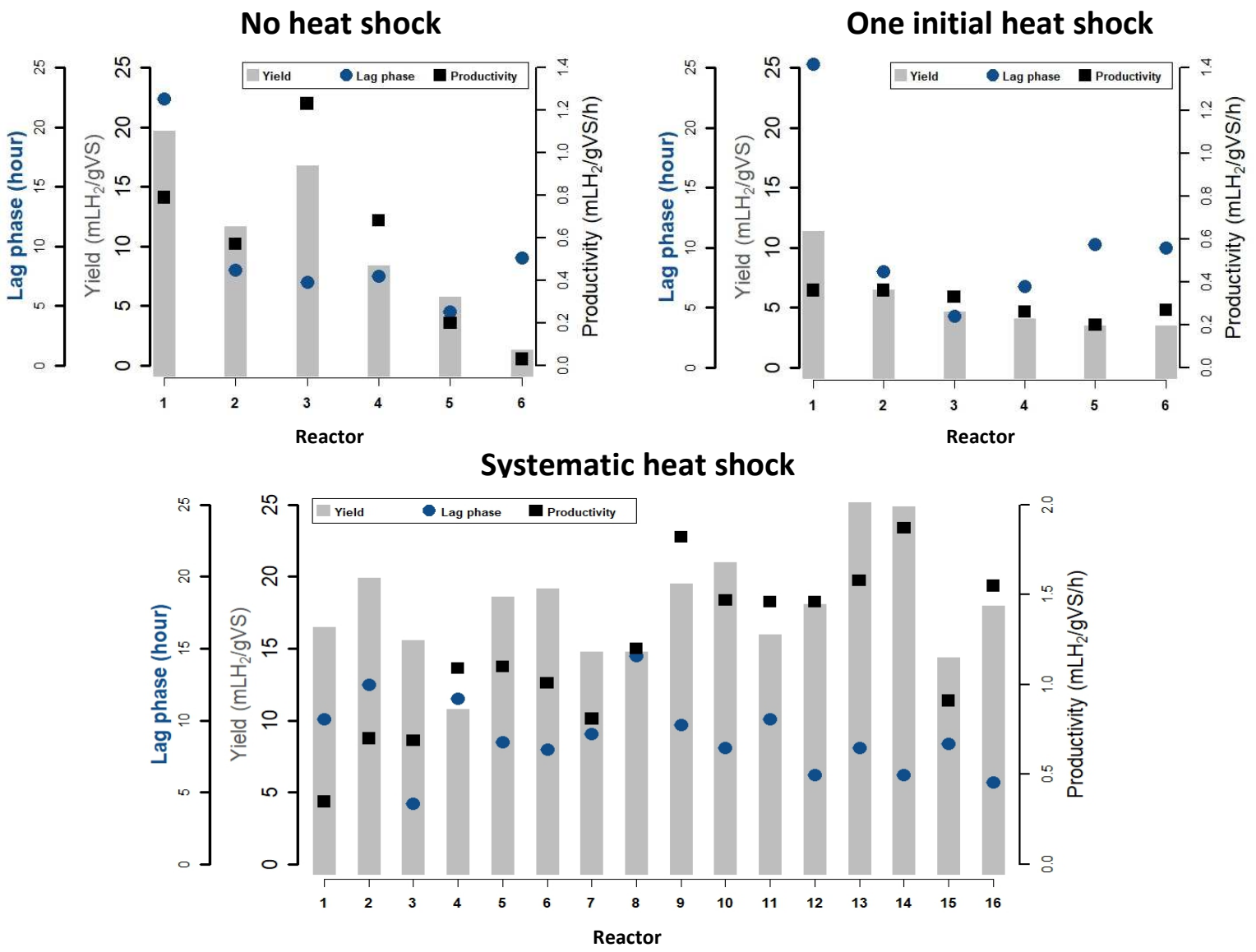
No heat shock
One initial heat shock
Systematic heat shock
Yield
Lag phase
Productivity
Lag phase (hour)
Yield (mLH2/gVS)
Productivity (mLH2/gVS/h)
Reactor

Fig. 3.

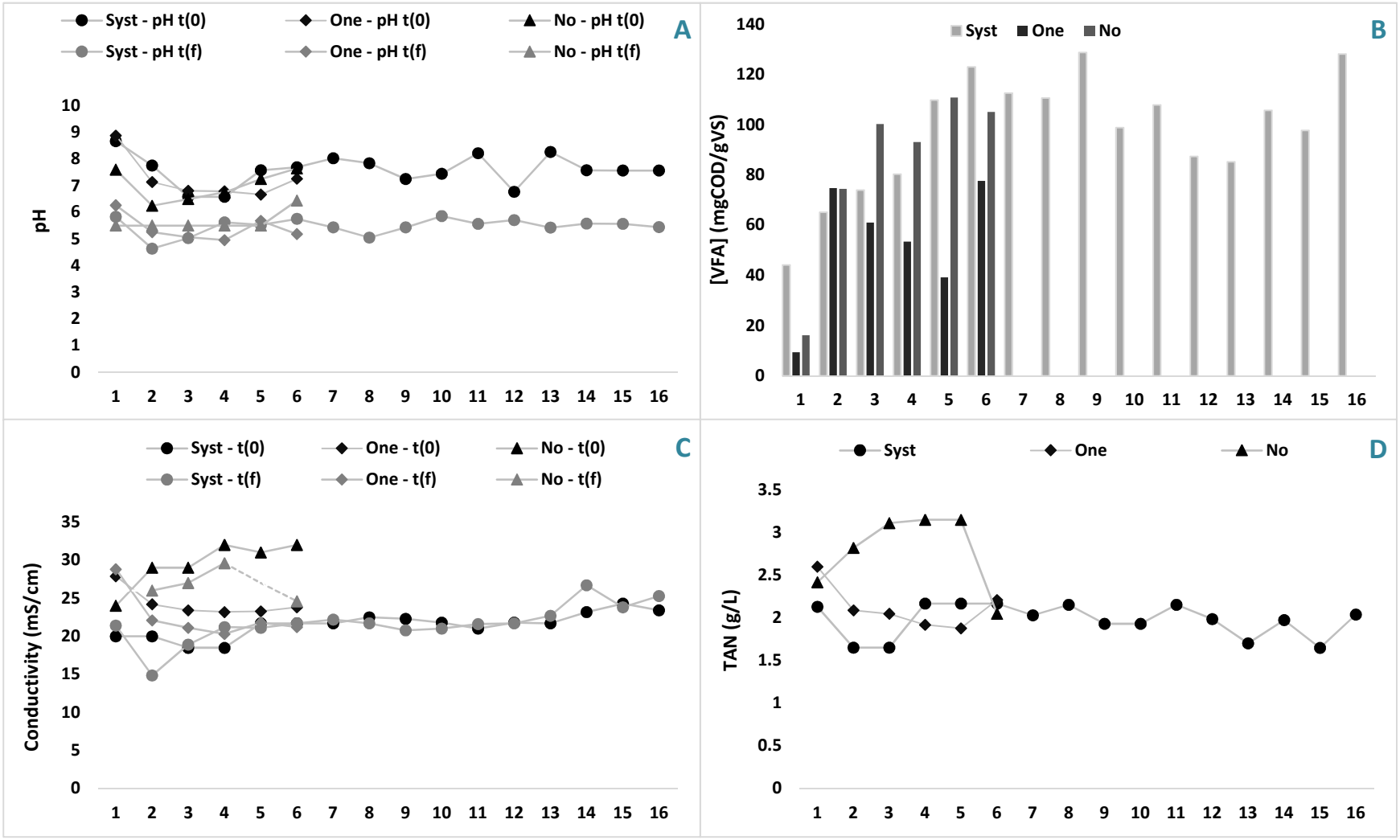
A
Syst - pH t(0)
One - pH t(0)
No - pH t(0)
Syst - pH t(f)
One - pH t(f)
No - pH t(f)
pH
B
Syst
One
No
[VFA] (mgCOD/gVS)
C
Syst - t(0)
One - t(0)
No - t(0)
Syst - t(f)
One - t(f)
No - t(f)
Conductivity (mS/cm)
D
Syst
One
No
TAN (g/L)

Fig. 4.

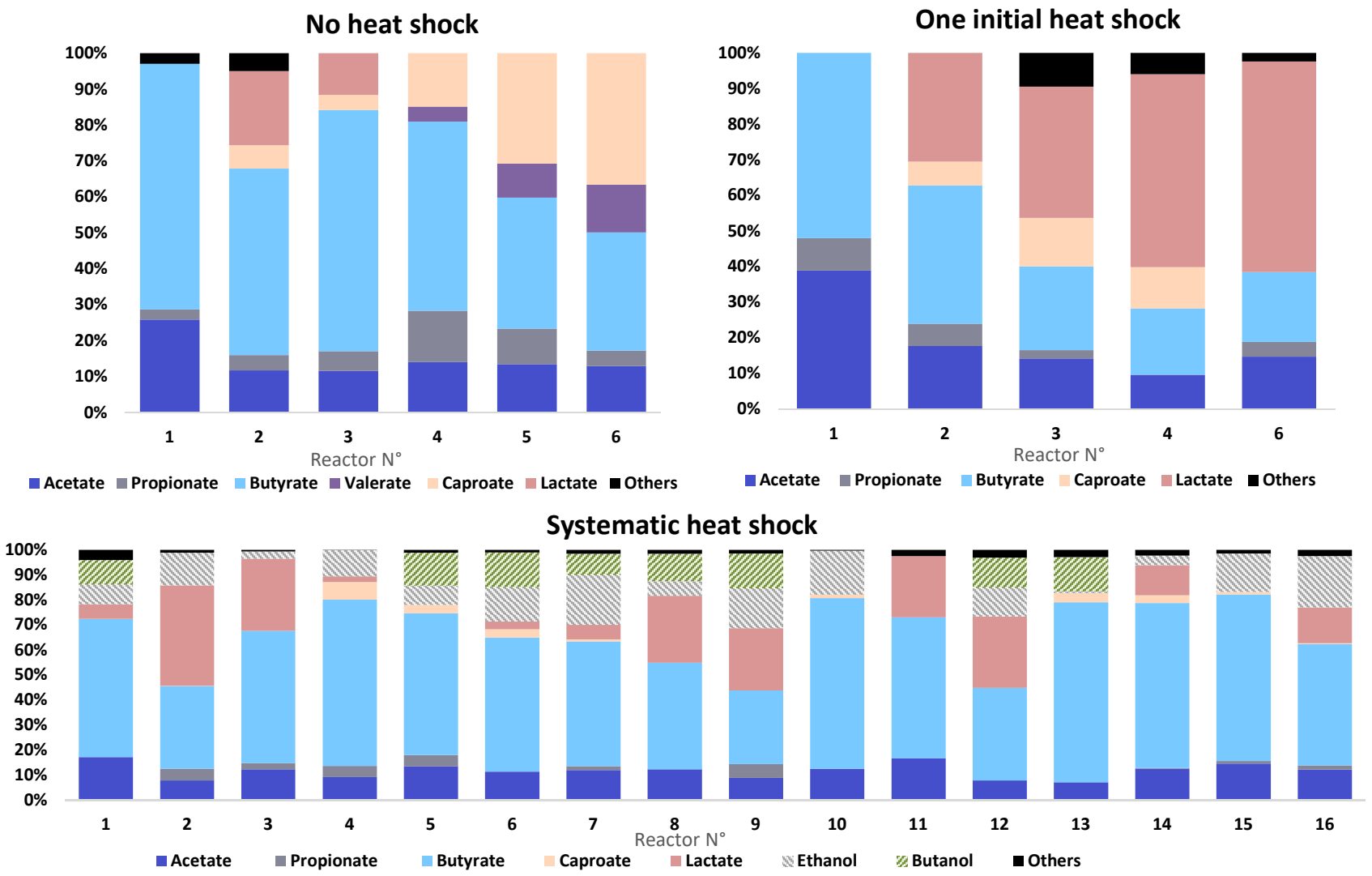
No heat shock
100%
90%
80%
70%
60%
50%
40%
30%
20%
10%
0%
1
2
3
4
5
6
Reactor N°
Acetate
Propionate
Butyrate
Valerate
Caproate
Lactate
Others
One initial heat shock
100%
90%
80%
70%
60%
50%
40%
30%
20%
10%
0%
1
2
3
4
6
Reactor N°
Acetate
Propionate
Butyrate
Caproate
Lactate
Others
Systematic heat shock
100%
90%
80%
70%
60%
50%
40%
30%
20%
10%
0%
1
2
3
4
5
6
7
8
9
10
11
12
13
14
15
16
Reactor N°
Acetate
Propionate
Butyrate
Caproate
Lactate
Ethanol
Butanol
Others

Fig. 5.

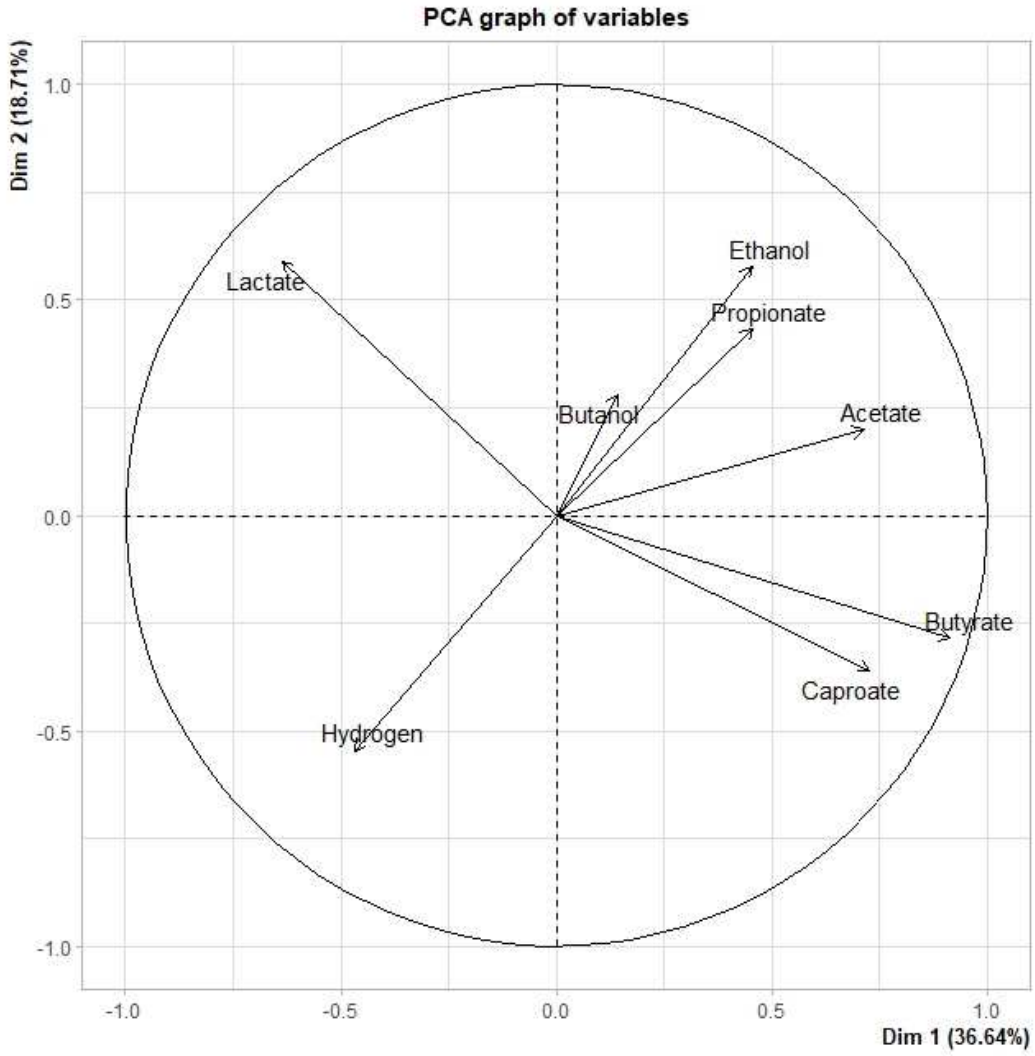
PCA graph of variables
Dim 2 (18.71%)
Dim 1 (36.64%)
1.0
0.5
0.0
-0.5
-1.0
-1.0
-0.5
0.0
0.5
1.0
Lactate
Ethanol
Propionate
Butanol
Acetate
Butyrate
Caproate
Hydrogen

Fig. 6.

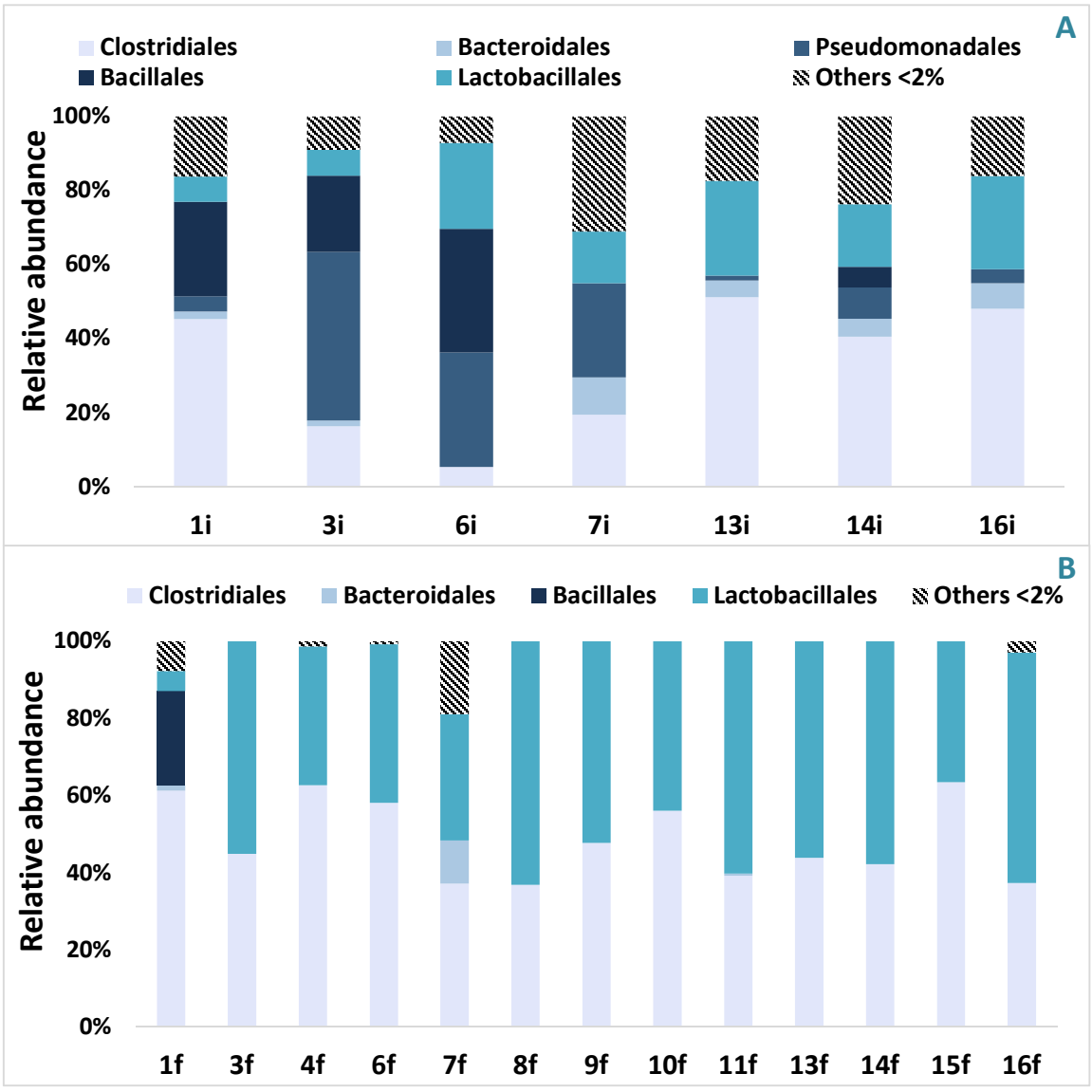
A
Clostridiales
Bacteroidales
Pseudomonadales
Bacillales
Lactobacillales
Others <2%
Relative abundance
100%
80%
60%
40%
20%
0%
1i
3i
6i
7i
13i
14i
16i
B
Clostridiales
Bacteroidales
Bacillales
Lactobacillales
Others <2%
Relative abundance
100%
80%
60%
40%
20%
0%
1f
3f
4f
6f
7f
8f
9f
10f
11f
13f
14f
15f
16f